Unraveling the Differences of the Hydrolytic Activity of *Trypanosoma cruzi trans*-Sialidase and *Trypanosoma rangeli* Sialidase: A Quantum Mechanics−Molecular Mechanics Modeling Study

Juan A. Bueren-Calabuig,[†,§] Gustavo Pierdominici-Sottile,[‡] and Adrian E. Roitberg*[,†]

[†]Department of Chemistry, Quantum Theory Project, University of Florida, Gainesville, Florida 32611, United States
[‡]Universidad Nacional de Quilmes, Roque Saenz Peña 352, B1876BXD Bernal, Argentina

ABSTRACT: Chagas' disease, also known as American trypanosomiasis, is a lethal, chronic disease that currently affects more than 10 million people in Central and South America. The *trans*-sialidase from *Trypanosoma cruzi* (*T. cruzi*, TcTS) is a crucial enzyme for the survival of this parasite: sialic acids from the host are transferred to the cell surface glycoproteins of the trypanosome, thereby evading the host's immune system. On the other hand, the sialidase of *T. rangeli* (TrSA), which shares 70% sequence identity with TcTS, is a strict hydrolase and shows no *trans*-sialidase activity. Therefore, TcTS and TrSA represent an excellent framework to understand how different catalytic activities can be achieved with extremely similar structures. By means of combined quantum mechanics−molecular mechanics (QM/MM, SCC-DFTB/Amberff99SB) calculations and umbrella sampling simulations, we investigated the hydrolysis mechanisms of TcTS and TrSA and computed the free energy profiles of these reactions. The results, together with our previous computational investigations, are able to explain the catalytic mechanism of sialidases and describe how subtle differences in the active site make TrSA a strict hydrolase and TcTS a more efficient *trans*-sialidase.
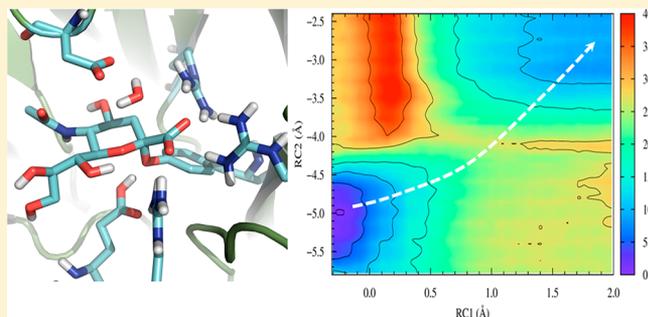
INTRODUCTION

American trypanosomiasis, also known as Chagas' disease, is caused by the parasite *Trypanosoma cruzi* (*T. cruzi*) and is considered by the World Health Organization (WHO) to be one of the 17 neglected tropical diseases. It is endemic in Central and South America where it affects 10−12 million people, killing over 15,000 each year and infecting hundreds of thousands worldwide.[1,2] It is transmitted to humans through the feces of triatomine bugs known as "kissing bugs", and also between humans by blood transfusion and from mother to infant.[3] The acute phase of the disease is usually asymptomatic while the chronic phase is characterized by the development of cardiac and digestive pathologies.[2,3] While most trypanosomatid parasites remain in blood, *T. cruzi* is an intracellular parasite. This fact seriously hinders the development of drugs for the treatment of Chagas disease.[4−8] To date, Nifurtimox and Benznidazole, are the only two approved drugs for the treatment of the infection despite their low efficacy and their severe side effects.[9] Consequently, investigations of new and more effective drugs as well as the characterization of novel targets are required. The *trans*-sialidase from *T. cruzi* (TcTS) is essential for the parasite infectivity in the human body, and combined with the fact that TcTS is not present in humans, it is currently considered a promising biochemical target for developing new molecules to control Chagas' disease.[10−16]

Sialic acids are O- and N-substituted derivatives of neuraminic acid, a nine-carbon monosaccharide, usually located on cell surface glycoproteins and glycolipids. These acids play a key role in biology by regulating antigenic expression and molecular interactions and providing structural support and protection to cell membranes.[17−19] Sialidases are a family of enzymes that catalyzes the removal of sialic acid from various glycoconjugates and constitute virulence factors of numerous viruses and prokaryotic and eukaryotic microorganisms.[20] These enzymes are expressed in different parasites including *Trypanosoma brucei*, the causative agent of African Trypanosomiasis, Trypanosoma rangeli (*T. rangeli*), and *T. cruzi*. Both the sialidase of *T. rangeli* (TrSA) and TcTS are part of the sialidase family, but while the former is a strict hydrolase, the latter preferentially displays a *trans*-sialidase activity catalyzing the transfer of sialic acid residues from the host glycoconjugates to the parasite surface mucins.[12,21,22] As a result, the parasite is protected from the host's immune system and gains the ability to adhere to and invade host cells.[23]

TcTS and TrSA have a 70% sequence identity and the overall C_α root mean squared deviation (RMSD) value is only 0.59 Å. Both enzymes fold into two structural domains. The N-terminal catalytic domain shows a β-propeller fold which is connected by a long α-helical segment to the C-terminal domain displaying a β-barrel lectin-like topology.[24,25] Despite the high structural

Scheme 1. Mechanisms Showing the Transfer (Top) And Hydrolysis (Bottom) Reactions[a]
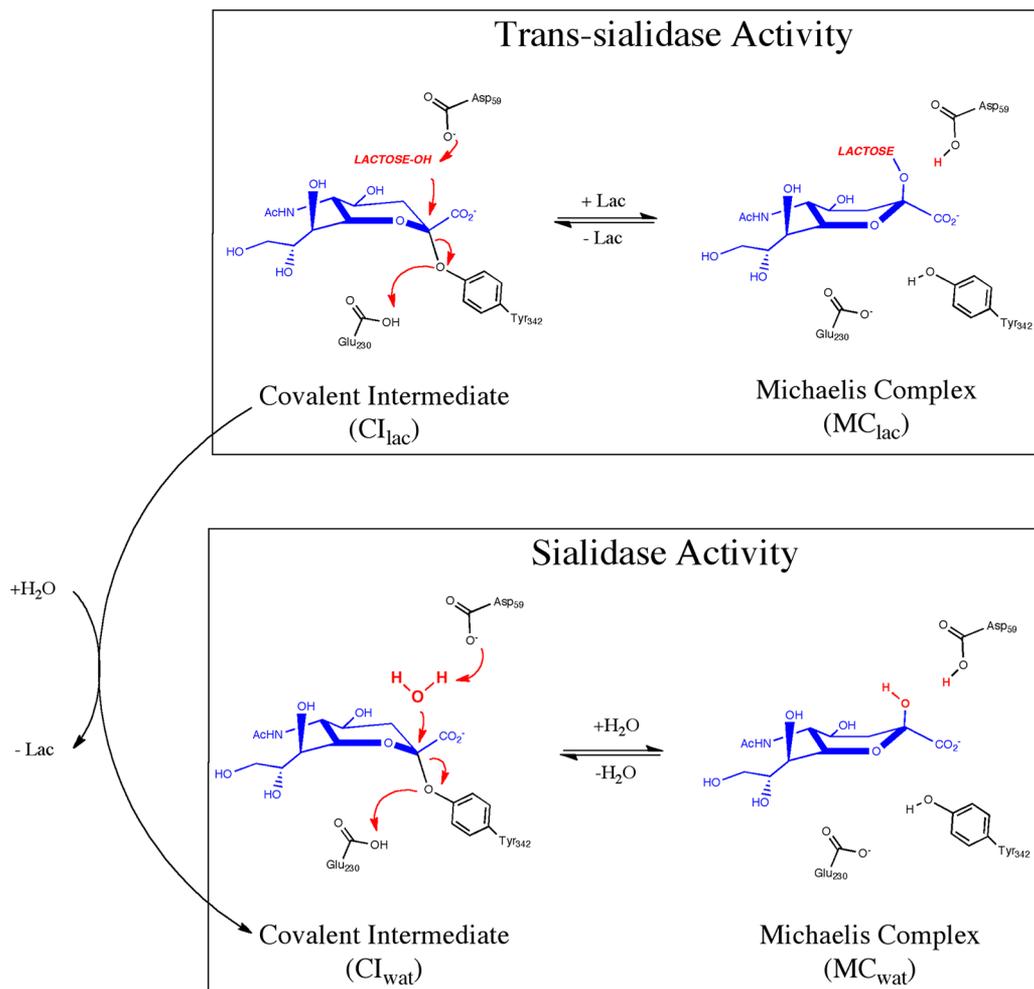
[a]Once the CI_{lac} is obtained, only TcTS is able to transfer sialic acid to the parasite lactose-containing mucins leading to the MC_{lac}. If the lactose group in the CI_{lac} is replaced by a water molecule at the active site of the enzyme, the newly established CI_{wat} is hydrolyzed by a water molecule to MC_{wat}. TrSA is a very efficient hydrolase while TcTS preferentially shows *trans*-sialidase activity.

similarity, no *trans*-sialidase activity is present in TrSA, which exclusively catalyzes the hydrolysis of sialic acid residues from sialyl-glycoconjugates.[25,26] Furthermore, good inhibitors of TrSA (e.g., DANA and tamiflu) are only very weak inhibitors of TcTS,[24,25,27] indicating that small differences in the sequence and structure can give rise to substantial changes in the catalytic mechanism.

In this work, the residue numbers of both TrSA and TcTS will be referred to those of the crystal structure of the TcTS complex with sialyllactose (PDB ID: 1S0I).[28] The active sites of TcTS and TrSA contain several residues conserved in other microbial sialidases. Those active site residues include the following: the catalytic residues Tyr342, Glu230, and Asp59 (involved in proton shuffling and nucleophilic attack); an arginine triad (Arg35, Arg245, and Arg314), which interacts with the carboxylate group of the sialic acid; and Asp96, which is H-bonded with O11 and N12 of sialic acid. In addition, in TcTS, Trp312 and Tyr119 display a hydrophobic lactose-binding region. In TrSA, Tyr119 is substituted by Ser119 leading to a less suitable region for the accommodation of the lactose ring.

The catalytic mechanisms of the hydrolysis and transfer reaction are depicted in Scheme 1.

Structural and kinetic studies revealed a double-displacement (ping-pong) mechanism with formation of a covalent sialyl-enzyme intermediate via Tyr342.[28−32] After the formation of the Michaelis complex in the presence of lactose (MC_{lac}), both enzymes are able to cleave the host sugar−sialic acid bond leading to the covalent intermediate, with the leaving group (donor sugar) still present at the active site (CI_{lac}). Once the CI_{lac} is reached, TcTS completes its *trans*-sialidase activity by taking the reverse step but in this case transferring the sialic acid to a parasite sugar (acceptor group) leading to a new MC_{lac}. In this reaction, the anomeric carbon of the sialic acid is attacked by the lactose hydroxyl oxygen, which is deprotonated by Asp59 while the Tyr342 phenolic oxygen is protonated by Glu230. In contrast, TrSA is unable to achieve the transfer reaction of sialic acid to the parasite surface glycoconjugates. In this case, the donor sugar in CI_{lac} is replaced by a water molecule (CI_{wat}). The hydrolysis of CI_{wat} to MC_{wat} is achieved by a nucleophilic water attack. Although this second path can be accomplished by both enzymes, TcTS was shown to be significantly more efficient in transferring than in hydrolyzing sialic acids.[25]

A great deal of effort has been applied to identify the determinants of the *trans*-sialidase activity in TcTS in contrast
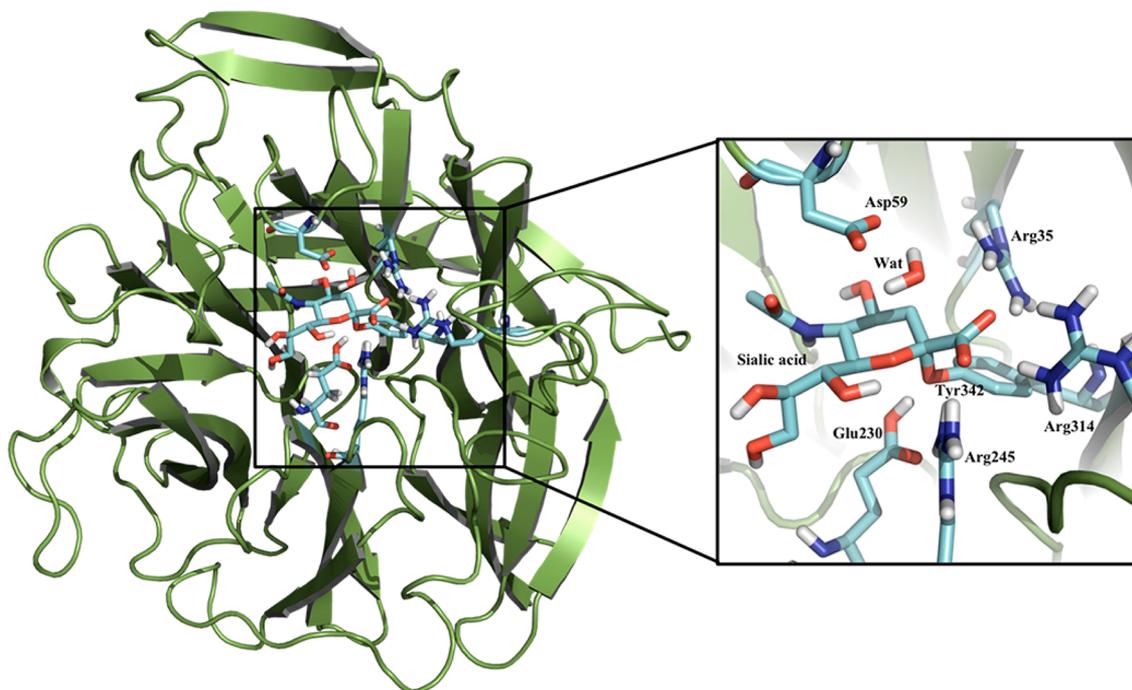
Figure 1. Representative structure of the TcTS covalent intermediate (CI_{wat}) used as the starting point for the umbrella sampling simulations. The amino acids included in the classical MM region are shown in green while the QM residues are displayed in light blue sticks. For clarity, only the polar hydrogen atoms are represented.

with the strict hydrolase activity of TrSA.[11,25,33−35] The active site of TcTS shows a narrower and more hydrophobic binding pocket than TrSA. This was confirmed by molecular dynamics (MD) simulations performed by our group that showed that the TrSA CI_{wat} adopted a more open catalytic cleft compared to that of the TcTS, facilitating the access of water molecules.[36] Therefore, the *trans*-sialidase activity in TcTS can, in part, be favored by the exclusion of water molecules and the establishment of nonpolar interactions between the active site residues and the lactose group.[24,37] Moreover, we have recently found that when lactose is not present in the active site, the catalytic couple Tyr342-Glu230 is dissociated when TcTS is found in its covalent intermediate (CI) form. However, that behavior was not observed in TrSA.[38] These facts support the idea of a long-lived CI that could be involved in the sialyl-transfer mechanism of TcTS.[28,39,40] Recently, five TrSA key residues were mutated by Paris et al. (Met95-Val, Ala97-Pro, Ser119-Tyr, Gly248-Tyr and Gln283-Pro) leading to a quintuple mutant that showed around 1% *trans*-sialidase activity.[27] However, despite the numerous experimental and theoretical studies carried out thus far, the reasons for the different catalytic activities between both enzymes are still unclear.

Molecular modeling has become one of the most important tools to gain atomic insight and quantitative understanding of enzymatic reactions.[41] Computational enzymology provides detailed features of the reaction pathways acting as a complement to experimental techniques.[42,43] Recently, we studied the CI_{lac} formation in TcTS[34] and in TrSA, together with specific mutations that provided important insight into the *trans*-sialidase activity.[33] In the present work, the hydrolytic activity of TcTS and TrSA was modeled using computer simulations and free energy calculations in order to complete the mechanistic studies in TcTS and TrSA and rationalize their distinct catalytic behavior.

METHODS

Setup of the Covalent Intermediate Models. MD simulations of the CI_{wat} of TrSA and TcTS (PDB IDs: 2A75 and 2AH2, respectively) were performed by our group and described in previous work.[36] Representative conformations of TcTS and TrSA from unrestrained MD simulations were used as initial structures for the quantum mechanics/molecular mechanics (QM/MM) umbrella sampling simulations. Those systems included a water molecule present at a location suitable for the nucleophilic attack. In this conformation, a hydrogen bond is established between the water molecule and the carboxylic group of Asp59. The distance between the oxygen atom of the water molecule and the anomeric C in both covalent intermediates is less than 4 Å and an average hydroxyl oxygen (Tyr342)−anomeric C (sialic acid)−O (water) angle of approximately 170° suggested an ideal position for an in-line attack on the anomeric C (sialic acid)−hydroxyl oxygen (Tyr342) bond.

QM/MM Umbrella Sampling Simulations. Classical molecular mechanics can provide atomic insight into the active site of enzymes and contribute to identifying the determinants of reactivity. However, they are unable to treat processes taking place during enzymatic reactivity, including bond formation and breaking.[44] In the hybrid QM/MM approach, the reactive part is treated using quantum mechanics while the rest of the system is treated with a classical force field (MM).[41,45]

For each CI_{wat}, the QM region included Glu230, Asp59, sialic acid, Tyr342, Arg245, Arg314, and Arg35 and the water molecule while the rest of the enzyme residues were treated using the Amber99SB force field (Figure 1).[46,47]

Hydrogen link atoms were used to treat the covalent bonds between the side chain of the catalytic residues (QM region) and the backbone of the protein (MM region). The self-consistent charge density functional tight binding (SCC-

DFTB) method, as implemented in AMBER,[48] was employed to study the quantum region. SCC-DFTB was used successfully in many biomolecular simulations and chemical reactions[49−51] and was found to be in good agreement with QM/MM calculations developed at higher levels of QM theory, such as MP2.[52] This method was also shown to provide the best semiempirical description of five- and six-membered carbohydrate ring deformations.[53] We have previously shown that the energy barriers obtained using DFTB and MP2 for the *trans*sialidase activity of TcTS are very similar.[34]·

The reactions of the hydrolysis of the CI_{wat} to MC_{wat} were modeled by means of umbrella sampling using conditions similar to those previously used in TcTS.[34,54] The distances involved in defining the reaction coordinates (denoted as RC1 and RC2) are depicted in Scheme 2.

Scheme 2. Illustration of the Reaction Coordinates Chosen To Simulate the Hydrolysis of the Sialyl-Enzyme Covalent Intermediate[a]
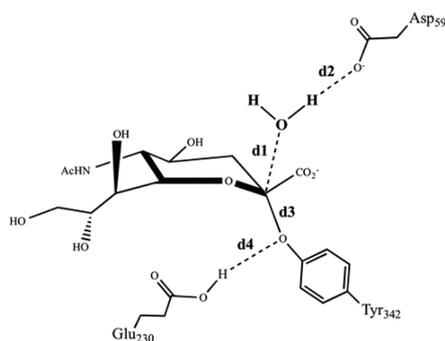
[a]The 2-D reaction coordinate is defined by RC1 and RC2: RC1 = d_3 − d_4 and RC2 = −d_1 − d_2.

d_1 refers to the distance between the anomeric carbon and the catalytic water oxygen while d_2 refers to the distance between a Asp59 carboxylic oxygen and the nearest water hydrogen. d_3 refers to the distance between the anomeric carbon and the Tyr342 hydroxyl oxygen, and d_4 corresponds to the distance between one Glu230 carboxylic oxygen and the Tyr342 hydroxyl oxygen. A combination of two reaction coordinates was used to model the reaction: RC1 represents the cleavage of the sialic acid−Tyr342 bond and the protonation of the tyrosine by abstracting a proton from the Glu230 oxygen: RC1 = d_3 − d_4. RC2 describes the deprotonation of the water molecule by an Asp59 oxygen and the subsequent attack of the oxygen to the anomeric carbon of the sialic acid: RC2 = −d_1 − d_2. RC1 was harmonically restrained from −0.30 to 2.10 Å while RC2 was restrained from −5.9 to −2.4 Å. The scans were completed using 0.08 Å steps with a force constant of 450.0 kcal/(mol·A²). The total number of windows in the 2-D umbrella calculation was around 1300. For each QM/MM simulation 2 ps was considered to equilibrate the system before running 20 ps in the production phase. For every MD simulation, periodic boundary conditions with a cutoff distance of 12.0 Å and a time step of 1.0 fs were used. The particle mesh Ewald method was used to calculate the long-range Coulomb forces.[55] The 2-D weighted histogram analysis method (WHAM-2D)[56] was used to unbias the simulations and to obtain the free energy surface (FES) along the reaction coordinates following the same protocol used for the study of the *trans*-sialidase activity of

TcTS.[34] The minimum free energy path (MFEP) is identified by following the path connecting the energy minima through the transition state (TS) that is orthogonal to the equipotential contours of the FES.[57]

Energy Decomposition Analysis. The energy decomposition method was employed to investigate the functional roles of TcTS and TrSA active site residues during the hydrolysis of the sialic acid CI_{wat}. This method has been widely applied to identify the importance of different amino acids in the catalytic mechanism of enzymes[58−65] and was recently employed by our group in different studies.[34,54] We used it here to investigate the stabilization pattern of TcTS and TrSA residues on TS_{wat} with respect to the CI_{wat}. The QM region included the catalytic residues Asp59, Glu230, and Tyr342, a water molecule, and the sialic acid. A total of 400 configurations in the CI_{wat} and TS_{wat} configurations were selected in each case. For each configuration, every residue from the MM subsystem within 10 Å to the sialic acid was individually mutated to Gly. The averaged quantum mechanical energy was computed in each step in the wild-type proteins and for each mutant structure. The influence of a particular residue on the energy of a particular conformation was measured taking into account the difference of energies when a particular residue is present (denoted by i in eq 1) or when it is replaced by Gly ($i − 1$ in eq 1).

$$\Delta E_i = [E_i^{QM} + E_i^{QM/MM}] − [E_{i-1}^{QM} + E_{i-1}^{QM/MM}] \qquad (1)$$

The contribution of each residue to the stabilization of TS_{wat} during the hydrolysis of the CI_{wat} to the MC_{wat} was obtained by measuring the difference between the stabilization patterns of these residues in TS_{wat} and CI_{wat},

$$\Delta\Delta E_i = \Delta E_i^{TS_{wat}} − \Delta E_i^{CI_{wat}} \qquad (2)$$

Thus, a positive/negative value of $\Delta\Delta E_i$ indicates that residue i exerts a higher destabilization/stabilization electrostatic effect on TS_{wat} than on CI_{wat}. This selective stabilization pattern occurs because the analyzed residue adjusts its position and/or because the electrostatic distribution of the QM subsystem changes when the system goes from CI_{wat} to TS_{wat}. Thus, the $\Delta\Delta E$ values represent useful information on how the enzyme selectively stabilizes a particular state (i.e., TS_{wat}) with respect to another. It should be noted that the relationship between the $\Delta\Delta E$ and how a mutation can help to further stabilize the reaction is not direct. In fact, if we modified a specific residue, not only the electronic distribution of the QM subsystem, but also the positioning of the other residues are affected, and thus all of the pattern is modified.

More O'Ferral−Jencks Diagram. In order to describe the mechanism, a reaction space plot based on a two-dimensional More O'Ferral−Jencks diagram[66] was created for both TrSA and TcTS enzymatic reactions. The reactant (CI_{wat}) is located on the lower left corner, the product is on the upper right, and the x and y axes represent the Pauling bond order[67] along the MFEP for O (water)−sialic acid bond making and the breaking of the sialyl−Tyr342 bond, respectively. The Pauling bond order, n_x, was determined using the following equation:[68]

$$n_x = n_0 \exp\left[\frac{(R_0 − R_x)}{0.6}\right]$$

where n_0 denotes the bond order of the fully formed bond of length R_0 (in this case R_0 = 1.4 Å, and n_0 = 1) and R_x is the
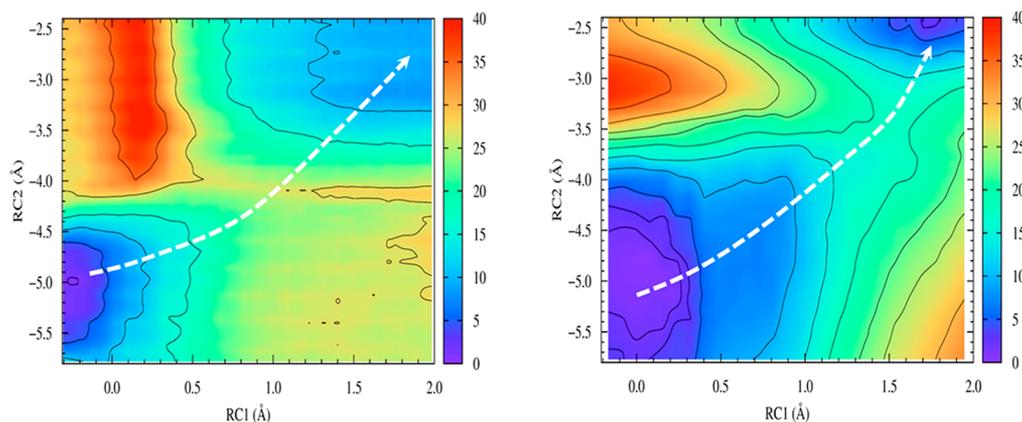
Figure 2. Free energy surfaces for the hydrolysis of the CI_{wat} catalyzed by TcTS (left) and TrSA (right). Results are in kilocalories per mole. The white dashed lines illustrate the minimum energy path to reach MC_{wat} from CI_{wat}.

average distance between the leaving group (Tyr342) or nucleophile (water) and the anomeric C.

Analysis of the Molecular Dynamics Trajectories. Three-dimensional structures and trajectories were visually inspected by using the computer graphics program PyMOL.[69] Interatomic distances and angles were monitored by using the *ptraj* module in AmberTools 12.[70,71]

■ RESULTS AND DISCUSSION

Description of the Hydrolysis Mechanism. The analysis of the 2-D FES describing the hydrolysis of the CI_{wat} by TcTS and TrSA showed a clear MFEP connecting CI_{wat} to MC_{wat} (Figure 2).

For both enzymes MFEPs proceed diagonally indicating that the reaction coordinates RC1 (involving Tyr342−sialic acid bond cleavage) and RC2 (associated with the water activation and nucleophilic attack on the anomeric C) are highly correlated. To better describe the mechanism, a "reaction space" plot, based on a More O'Ferrall−Jencks style diagram, is presented in Figure 3.[66]

For both systems, at the transition state (TS_{wat}), the Tyr342−sialic acid bond is almost cleaved (Pauling bond order ∼ 0.1) while the C_{sial}−O_{wat} bond formation is beginning (Pauling bond order ∼ 0.26), showing that the hydrolysis reaction follows an A_ND_N mechanism of dissociative type.[72]
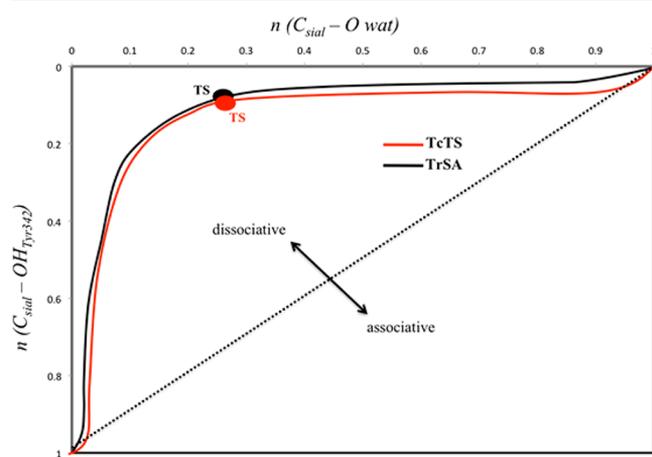
Figure 3. Reaction space for the hydrolysis of the CI_{wat} during the sialidase activity of TcTS (red) and TrSA (black).

Interestingly, the same behavior was observed for the *trans*-sialidase activity of both enzymes.[33,34] Taking into account all of these data, it can be concluded that, for TcTS and TrSA, the mechanism is A_ND_N dissociative, regardless of the nature of the nucleophile or the leaving group. In others words, the sialidase and *trans*-sialidase activities share a common mechanism in both cases.

The last paragraph highlights common features of the hydrolysis mechanism of TcTS and TrSA. However, it is worth noticing some subtle aspects that differ, such as the conformations of the reaction critical points, depicted in Figure 4.

The initial CI_{wat} displays a very similar structure between TcTS and TrSA. The water molecule is hydrogen-bonded to Asp59 and is suitably positioned for a nucleophilic attack to the sialic acid anomeric carbon. At the TS_{wat}, Tyr342 is no longer bound to sialic acid and its hydroxyl oxygen is protonated by Glu230. A hydrogen bond is still present between the water molecule and Asp59, but the covalent bond with the sialic acid is not yet formed. The important distances at the critical points are summarized in Table 1.

At the TS_{wat}, the distance from the oxygen atom of the nucleophilic water molecule to the anomeric C of sialic acid is the same for TrSA and TcTS ($d_1 = 2.1$ Å). In contrast, d_2 is 0.4 Å shorter in TrSA than in TcTS, making the oxygen atom of the water molecule a better nucleophile in the former. At the TS_{wat} of both enzymes, the Tyr342−sialic acid bond is already cleaved and Tyr342 has accepted the proton from Glu230. This proton transfer is almost completely achieved in both TcTS and TrSA ($d_4 = 1.3$ and 1.2 Å, respectively).

Significant conformational changes of the sialic acid ring were observed during the hydrolysis of the CI_{wat} to MC_{wat}. In the CI_{lac}, the sialic acid adopted a $^2C_5$ (half-chair) conformation. The structures sampled at the TS_{wat} adopted a $^4H_5$ half-chair conformation where atoms O5, C1, C4, and C5 form the reference plane.[73] Finally, when the MC_{wat} is reached, the sialic acid ring conformation migrates to a $B_{2,5}$ boat. We can follow this process by computing the pyramidalization dihedral around the anomeric carbon of sialic acid (Figure 5).

The torsion moved from +40° (CI_{wat}) to −40° (MC_{wat}) describing a reverse conformation change compared to the one observed during the *trans*-sialylation reaction in TcTS, resulting in an overall retention of the configuration of the sialic acid ring.[25,34] The evolution of the anomeric C−O13 bond distance along the MFEP was also analyzed. The distance is shortened
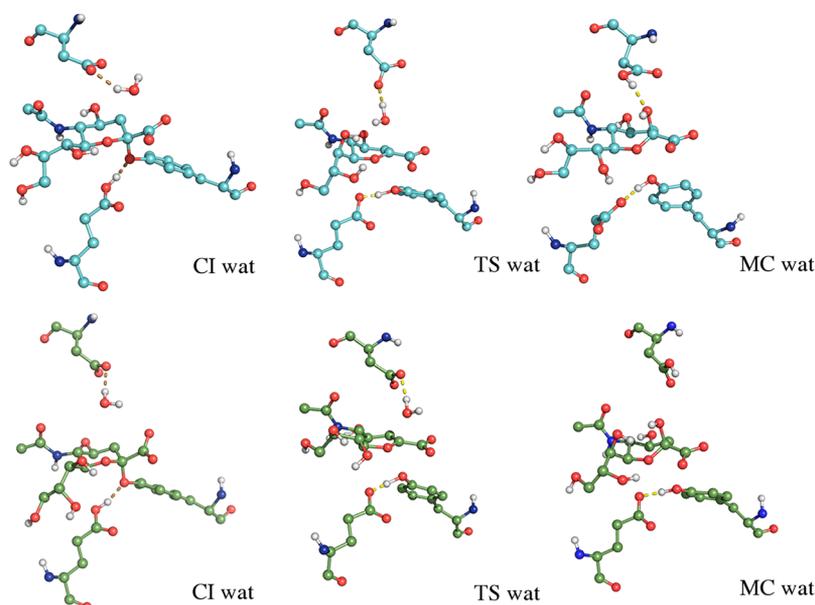
Figure 4. Structures obtained from the QM/MM umbrella sampling simulations corresponding to the covalent intermediate (CI_{wat}), transition state (TS_{wat}), and final Michaelis complex (MC_{wat}), for the hydrolysis of sialic acid catalyzed by TcTS (top) and TrSA (bottom).

Table 1. Average Reaction Coordinate Distances (Å) at MC_{wat}, TS_{wat}, and CI_{wat} in TcTS and TrSA[a]

	CI_{wat}[b]		TS_{wat}[c]		MC_{wat}[d]	
	TcTS	TrSA	TcTS	TrSA	TcTS	TrSA
d_1	3.1	3.2	2.1	2.1	1.4	1.4
d_2	2.1	2.1	1.8	1.4	1.0	1.0
d_3	1.4	1.4	2.5	2.7	3.1	3.1
d_4	1.7	1.5	1.3	1.2	1.0	1.0

[a]All standard deviations corresponding to these calculations were below 0.3 Å. [b]CI_{wat} = covalent intermediate. [c]TS_{wat} = transition state . [d]MC_{wat} = Michaelis complex.

gaining a partial double bond character at the TS_{wat}, after which the anomeric C−O13 bond recovers the single bond character reproducing the effects observed during the transfer activity in TcTS. This is the expected behavior for an oxocarbenium transition state.

Energy Profiles for TcTS and TrSA. The energy barrier ($\Delta G_r^{\ddagger}$) to reach the MC_{wat} from the CI_{wat} in TcTS is 26.8 kcal/mol, which is considerably higher than the barrier obtained for TrSA (16.4 kcal/mol), indicating that the hydrolysis of CI_{wat} is clearly more favored in TrSA. These data are in good agreement with the experimental evidence that identifies TrSA as a more efficient hydrolase than TcTS.[25] Although TrSA and TcTS share very similar structural components, the active site shows important differences that could account for the different hydrolysis rates of both enzymes. Moreover, the modifications observed in TcTS are able to overcome the fact that the water concentration in the active site is several orders of magnitude higher than that of lactose such that hydrolysis should be theoretically favored over the transfer reaction.[74]

The calculated energetic values of the hydrolysis catalyzed by TcTS can be compared with those from the *trans*-sialidase activity obtained in our previous works so that we can complete the rationale of the different activity of both enzymes (Figure 6).

In TcTS, the calculated energy barrier to bind a second lactose to the covalent intermediate during the *trans*-sialidase
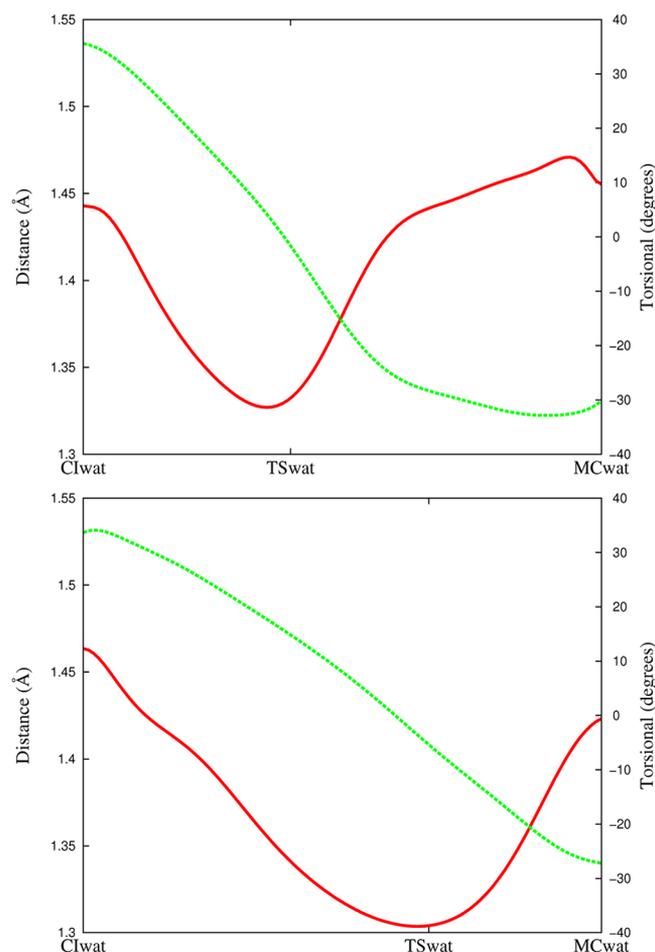
Figure 5. Anomeric C−O13 distance (red) and C9 (anomeric C)−C10−O13−C19 dihedral angle (green) along the minimum free energy path in TcTS (top) and TrSA (bottom). Atom names correspond to those in the PDB file.
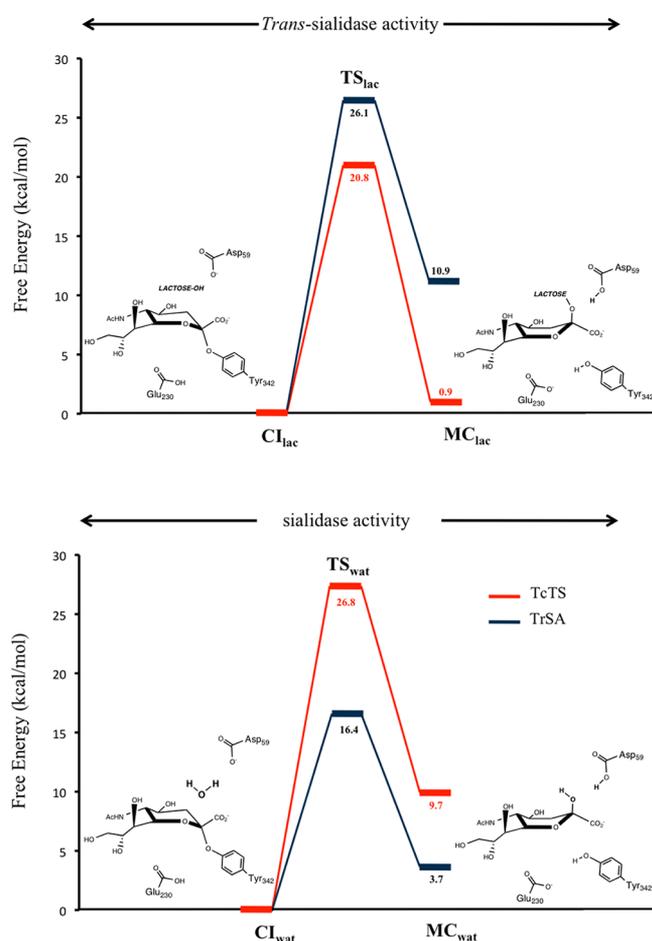
Figure 6. Free energy profiles for the *trans*-sialidase (top) and sialidase (bottom) activities catalyzed by TcTS and TrSA.

behaves as a strict hydrolase. Moreover, as it was shown for TcTS, the formation of a CI in TrSA is favored due the lower energy barriers calculated to reach the CI from the MC. In TrSA however, the reaction will proceed following the hydrolysis pathway.

The *trans*-sialidase activity energy values of TcTS were also compared to the hydrolysis activity measurements in TrSA. According to experimental data, the hydrolysis activity of TrSA is around twice the *trans*-sialylation rate catalyzed by TcTS.[25] Our theoretical data also support these conclusions since the energy barrier of the TrSA hydrolysis is 4 kcal/mol lower than TcTS *trans*-sialylation and the final products of the reaction have similar energies.

Energy Decomposition. Finally, the energy decomposition method was employed to identify the influence of individual active site residues on the energy barrier of the hydrolysis of the CI_{wat} (Figure 7).
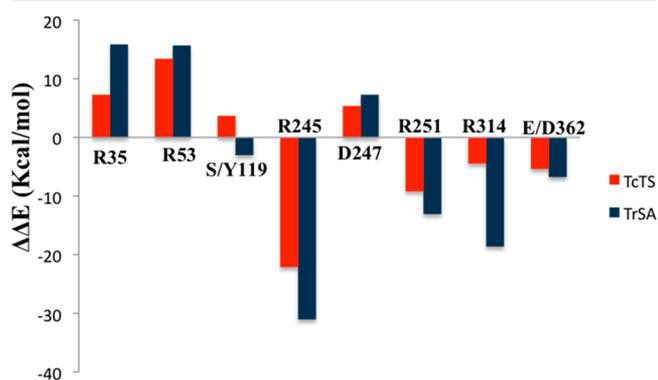
Figure 7. Relative stabilization pattern of the most relevant active site residues on the TS_{wat} considering the CI_{wat} as reference.

reaction is 20.8 kcal/mol—6 kcal/mol lower than the hydrolysis reaction. This agrees with the experimental findings confirming that TcTS behaves preferentially as a *trans*-sialidase rather than as a sialidase. Furthermore, the free energy difference (ΔG_r°) between the product of the hydrolysis (MC_{wat}) and reactant (CI_{wat}) in TcTS is 9.7 kcal/mol, indicating that the CI_{wat} is much more stabilized than the MC_{wat}. On the other hand ΔG_r° between the product of *trans*-sialylation (MC_{lac}) and the reactants (CI_{lac}) is 0.9 kcal/mol making the CI_{lac} approximately equienergetic with the MC_{lac}.[34] These values suggest that although TcTS can behave as a sialidase at a much lower rate, the formation and stabilization of a CI is strongly preferred over its hydrolysis to the MC_{wat}. These findings attest to the formation of a long-lived CI in TcTS as it is required during the *trans*-sialidase activity by retaining the sialic acid longer, which favors the binding of new lactose to sialic acid.

The hydrolysis and *trans*-sialylation energy barriers were also compared for TrSA. We noticed that the hydrolysis reaction barrier is roughly 10 kcal/mol lower than that of the transfer reaction. As a consequence, the hydrolysis in TrSA will be strongly preferred over the *trans*-sialylation. In addition, ΔG_r° between MC_{wat} and CI_{wat} is 3.7 kcal/mol, whereas ΔG_r° between MC_{lac} and CI_{lac} is 10.9 kcal mol^{-1}, making MC_{wat} a much more stable complex than MC_{lac} in TrSA. These results suggest that the reactions are kinetically controlled and explain why TrSA does not show any *trans*-sialidase activity and

As expected, all of the residues that showed a significant effect on the energy barrier had an opposite behavior to the one observed in our previous work during the formation of the CI_{lac} from the MC_{lac}.[54] The residues that stabilized the TS in one reaction are responsible for a destabilizing effect on the other and vice versa. This is due to the fact that the nucleophile and the leaving group are inverted in both reactions. In the former, the nucleophilic group was the Tyr342 hydroxyl and the leaving group was the lactose molecule. In the present study, a water molecule represents the nucleophile while Tyr342 is the leaving group. Two out of the three arginines (Arg245 and Arg314) of the arginine triad together with Glu362 considerably contribute to stabilize the TS_{wat} whereas Arg35 has a destabilizing effect. Two additional arginines, Arg53 and Arg251, also display an important effect, increasing and lowering the energy barrier, respectively. In addition, Asp247, which interacts with Arg245, has a significant destabilizing effect. All of those arginines remain hydrogen-bonded to the carboxylate group of the sialic acid except for Arg53, which is interacting with Asp59. The stabilizing or destabilizing behaviors brought about by those residues are common to both TrSA and TcTS although the effects are larger in TrSA, which can be explained considering the following facts. Configurations of the MC_{wat} complex of both TrSA and TcTS are very similar, but this is not the case for the TS_{wat} structures. As it was mentioned, d_2 is shorter for TrSA whereas d_3 is larger. Those differences account for a higher ionic character of both substrates in TrSA (i.e., the water molecule resembles more a hydroxyl group and the sialic acid

adopts a higher oxicarbenium character). As a consequence, the interaction between the active site residues and the enzyme substrates is stronger in TrSA than in TcTS which, in turn, is seen as a larger stabilizing/destabilizing effect of the common active site residues.

Important effects are observed in other residues from the catalytic cleft, though the contributions to the stability of the TS_{wat} are not as large as the ones presented by the former arginines. While TcTS has a tyrosine in position 119, TrSA contains a serine. Interestingly, Ser119 contributes to lowering the energy barrier in TrSA ($\Delta\Delta E = -3.0$ kcal/mol) while the tyrosine shows the opposite effect in TcTS ($\Delta\Delta E = +3.7$ kcal/mol). This finding, together with the fact that Ser119 favors the solvent exposure of the catalytic cleft and the stabilization of the water molecule in the active site of TrSA, helps to rationalize why TrSA strictly displays hydrolase activity, contrary to TcTS. Moreover, when Ser119 was mutated to tyrosine in TrSA, the sialidase activity was reduced by 50%.[25,75] On the contrary, in TcTS, the aromatic side chain of Tyr119, together with Trp312, forms a hydrophobic pocket that excludes water from the active site,[24] hindering the hydrolysis reaction on one hand and favoring the transfer activity on the other by establishing stacking interactions with the incoming lactose.

CONCLUSION

The CI_{wat} hydrolysis reactions catalyzed by TcTS and TrSA were simulated using QM/MM calculations combined with umbrella sampling simulations. The FES obtained showed a clear MFEP between reactants (CI_{wat}) and products (MC_{wat}). In both enzymes the reaction proceeds by means of a A_ND_N dissociative mechanism. The free energy calculations presented here together with our previous studies of the TS reactions allow us to obtain the following conclusions: (i) The estimated reaction barrier for the hydrolysis of the CI_{wat} by a water molecule catalyzed by TrSA is 16.4 kcal/mol, i.e., 10 kcal/mol lower than the same reaction catalyzed by TcTS (26.8 kcal/mol), and explains why TrSA is a more efficient hydrolase than TcTS. (ii) In TcTS, the energy barrier to accomplish the transfer reaction is 6 kcal/mol lower compared to the sialidase reaction. TcTS would then preferentially behave as a *trans*-sialidase rather than a sialidase. Moreover, the free energy difference also accounts for the establishment of a long-lived CI favoring the TcTS *trans*-sialidase activity. (iii) In TrSA, the hydrolysis reaction barrier is 10 kcal/mol lower than the transfer reaction, indicating that TrSA would have a more important role as a sialidase.

In addition, the energy decomposition allowed us to identify that, due to differential conformations, some residues (particularly Arg245 and Arg314) show a distinct stabilization pattern on TS_{wat} in TrSA and TcTS. Besides, the presence of Ser119 in TrSA slightly stabilizes the TS_{wat} while Tyr119 has the opposite effect in TcTS.

Besides the energetic dissimilarities shown above for the catalytic mechanism of TcTS and TrSA, other characteristics such as differential exclusion of water molecules from the active sites, stability of the active site residue conformations at the CI stage, and others aspects should also be considered to fully understand the distinctive properties of these highly similar enzymes.

Results presented here provide new insights into the catalytic mechanisms of TcTS and TrSA that complement our previous observations. Taken together, they help us to rationalize from different perspectives why TrSA behaves as a strict hydrolase

whereas TcTS preferentially acts a *trans*-sialidase. We hope this work can contribute to a deeper understanding of enzyme catalysis and to the development of new drugs leading to the inhibition of TcTS toward a possible treatment of the expanding Chagas' disease.

■ AUTHOR INFORMATION

Corresponding Author
*E-mail: roitberg@ufl.edu. Tel.: 352-392-6972.
Present Address
§EastCHEM School of Chemistry, The University of Edinburgh, Edinburgh EH9 3JJ, United Kingdom.
Notes
The authors declare no competing financial interest.

■ ACKNOWLEDGMENTS

■ REFERENCES

(1) Hotez, P. J.; Dumonteil, E.; Woc-Colburn, L.; Serpa, J. A.; Bezek, S.; Edwards, M. S.; Hallmark, C. J.; Musselwhite, L. W.; Flink, B. J.; Bottazzi, M. E. Chagas Disease: "The New HIV/AIDS of the Americas. *PLoS Neglected Trop. Dis.* **2012**, *6*, e1498.

(2) *American Trypanosomiasis: Chagas Disease One Hundred Years of Research*; Elsevier Insights, 1st ed.; Telleria, J., Tibayrenc, M., Eds.; Elsevier: London, 2010.

(3) Rassi, A.; Rassi, A.; Marin-Neto, J. A. Chagas Disease. *Lancet* **2010**, *375*, 1388−1402.

(4) Miller, B. R.; Roitberg, A. E. Trypanosoma Cruzi Trans-Sialidase as a Drug Target Against Chagas Disease (American Trypanosomiasis). *Future Med. Chem.* **2013**, *5*, 1889−1900.

(5) Clayton, J. Chagas Disease 101. *Nature* **2010**, *465*, S4−S5.

(6) Coura, J. R.; Castro, S. L. A Critical Review on Chagas Disease Chemotherapy. *Mem. Inst. Oswaldo Cruz* **2002**, *97*, 3−24.

(7) Tyler, K. M.; Engman, D. M. The Life Cycle of Trypanosoma Cruzi Revisited. *Int. J. Parasitol.* **2001**, *31*, 472−481.

(8) Andrews, N. W. Living Dangerously: How Trypanosoma Cruzi Uses Lysosomes to Get Inside Host Cells, and Then Escapes Into the Cytoplasm. *Biol. Res.* **1993**, *26*, 65−67.

(9) Cerecetto, H.; Gonzalez, M. Chemotherapy of Chagas Disease: Status and New Developments. *Curr. Top. Med. Chem.* **2002**, *2*, 1187−1213.

(10) Neres, J.; Brewer, M. L.; Ratier, L.; Botti, H.; Buschiazzo, A.; Edwards, P. N.; Mortenson, P. N.; Charlton, M. H.; Alzari, P. M.; Frasch, A. C.; et al. Discovery of Novel Inhibitors of Trypanosoma Cruzi Trans-Sialidase from in Silico Screening. *Bioorg. Med. Chem. Lett.* **2009**, *19*, 589−596.

(11) Neres, J.; Bryce, R. A.; Douglas, K. T. Rational Drug Design in Parasitology: Trans-Sialidase as a Case Study for Chagas Disease. *Drug Discovery Today* **2008**, *13*, 110−117.

(12) Buscaglia, C. A.; Campo, V. A.; Frasch, A. C. C.; Di Noia, J. M. Trypanosoma Cruzi Surface Mucins: Host-Dependent Coat Diversity. *Nat. Rev. Microbiol.* **2006**, *4*, 229−236.

(13) Pereira-Chioccola, V. L.; Acosta-Serrano, A.; Correia de Almeida, I.; Ferguson, M. A.; Souto-Padron, T.; Rodrigues, M. M.; Travassos, L. R.; Schenkman, S. Mucin-Like Molecules Form a Negatively Charged Coat That Protects Trypanosoma Cruzi Trypomastigotes From Killing by Human Anti-Alpha-Galactosyl Antibodies. *J. Cell Sci.* **2000**, *113* (Pt 7), 1299−1307.

(14) Pereira, M. E.; Zhang, K.; Gong, Y.; Herrera, E. M.; Ming, M. Invasive Phenotype of Trypanosoma Cruzi Restricted to a Population Expressing Trans-Sialidase. *Infect. Immun.* **1996**, *64*, 3884−3892.

5814

dx.doi.org/10.1021/jp412294r | *J. Phys. Chem. B* 2014, 118, 5807−5816

(15) Schenkman, S.; Eichinger, D.; Pereira, M. E.; Nussenzweig, V. Structural and Functional Properties of Trypanosoma Trans-Sialidase. *Annu. Rev. Microbiol.* **1994**, *48*, 499−523.

(16) Yoshida, N.; Mortara, R. A.; Araguth, M. F.; Gonzalez, J. C.; Russo, M. Metacyclic Neutralizing Effect of Monoclonal Antibody 10D8 Directed to the 35- and 50-kilodalton Surface Glycoconjugates of Trypanosoma cruzi. *Infect. Immun.* **1989**, *57* (6), 1663−1667.

(17) Schauer, R. Sialic Acids: Fascinating Sugars in Higher Animals and Man. *Zoology (Jena, Ger.)* **2004**, *107*, 49−64.

(18) Schauer, R. Achievements and Challenges of Sialic Acid Research. *Glycoconjugate J.* **2000**, *17*, 485−499.

(19) Varki, A. Sialic Acids as Ligands in Recognition Phenomena. *FASEB J.* **1997**, *11* (4), 248−255.

(20) Taylor, G. Sialidases: Structures, Biological Significance and Therapeutic Potential. *Curr. Opin. Struct. Biol.* **1996**, *6*, 830−837.

(21) Scudder, P.; Doom, J. P.; Chuenkova, M.; Manger, I. D.; Pereira, M. E. Enzymatic Characterization of Beta-D-Galactoside Alpha 2,3-Trans-Sialidase From Trypanosoma Cruzi. *J. Biol. Chem.* **1993**, *268*, 9886−9891.

(22) Ferrero-García, M. A.; Trombetta, S. E.; Sánchez, D. O.; Reglero, A.; Frasch, A. C.; Parodi, A. J. The Action of Trypanosoma Cruzi Trans-Sialidase on Glycolipids and Glycoproteins. *Eur. J. Biochem.* **1993**, *213*, 765−771.

(23) Schenkman, R. P.; Vandekerckhove, F.; Schenkman, S. Mammalian Cell Sialic Acid Enhances Invasion by Trypanosoma Cruzi. *Infect. Immun.* **1993**, *61*, 898−902.

(24) Buschiazzo, A.; Amaya, M. F.; Cremona, M. L.; Frasch, A. C.; Alzari, P. The Crystal Structure and Mode of Action of Trans-Sialidase, a Key Enzyme in. *Mol. Cells* **2002**, 1−12.

(25) Buschiazzo, A. Structural Basis of Sialyltransferase Activity in Trypanosomal Sialidases. *EMBO J.* **2000**, *19*, 16−24.

(26) Pontes-de-Carvalho, L. C.; Tomlinson, S.; Nussenzweig, V. Trypanosoma Rangeli Sialidase Lacks Trans-Sialidase Activity. *Mol. Biochem. Parasitol.* **1993**, *62*, 19−25.

(27) Paris, G.; Ratier, L.; Amaya, M. F.; Nguyen, T.; Alzari, P. M.; Frasch, A. C. A Sialidase Mutant Displaying Trans-Sialidase Activity. *J. Mol. Biol.* **2005**, *345*, 923−934.

(28) Amaya, M. F.; Watts, A. G.; Damager, I.; Wehenkel, A.; Nguyen, T.; Buschiazzo, A.; Paris, G.; Frasch, A. C.; Withers, S. G.; Alzari, P. M. Structural Insights Into the Catalytic Mechanism of Trypanosoma Cruzi Trans-Sialidase. *Structure* **2004**, *12*, 775−784.

(29) Davies, G. J.; Planas, A.; Rovira, C. Conformational Analyses of the Reaction Coordinate of Glycosidases. *Acc. Chem. Res.* **2012**, *45*, 308−316.

(30) Damager, I.; Buchini, S.; Amaya, M. F.; Buschiazzo, A.; Alzari, P.; Frasch, A. C.; Watts, A.; Withers, S. G. Kinetic and Mechanistic Analysis of *Trypanosoma cruzi* Trans-Sialidase Reveals a Classical Ping-Pong Mechanism with Acid/Base Catalysis. *Biochemistry* **2008**, *47*, 3507−3512.

(31) Watts, A. G.; Oppezzo, P.; Withers, S. G.; Alzari, P. M.; Buschiazzo, A. Structural and Kinetic Analysis of Two Covalent Sialosyl-Enzyme Intermediates on Trypanosoma Rangeli Sialidase. *J. Biol. Chem.* **2006**, 1−7.

(32) Watts, A. G.; Withers, S. G. The Synthesis of Some Mechanistic Probes for Sialic Acid Processing Enzymes and the Labeling of a Sialidase From Trypanosoma Rangeli. *Can. J. Chem.* **2004**, *82*, 1581−1588.

(33) Pierdominici-Sottile, G.; Palma, J.; Roitberg, A. E. Free-Energy Computations Identify the Mutations Required to Confer Trans-Sialidase Activity Into Trypanosoma Rangeli Sialidase. *Proteins* **2013**, DOI: 101002/prot24408.

(34) Pierdominici-Sottile, G.; Horenstein, N. A.; Roitberg, A. E. Free Energy Study of the Catalytic Mechanism of Trypanosoma Cruzitrans-Sialidase. From the Michaelis Complex to the Covalent Intermediate. *Biochemistry* **2011**, *50*, 10150−10158.

(35) Smith, L. E.; Eichinger, D. Directed Mutagenesis of the Trypanosoma Cruzi Trans-Sialidase Enzyme Identifies Two Domains Involved in Its Sialyltransferase Activity. *Glycobiology* **1997**, *7*, 445−451.

(36) Demir, O.; Roitberg, A. E. Modulation of Catalytic Function by Differential Plasticity of the Active Site: Case Study of *Trypanosoma Cruzi trans*-Sialidase and *Trypanosoma rangeli* Sialidase. *Biochemistry* **2009**, *48*, 3398−3406.

(37) Schauer, R.; Kamerling, J. P. The Chemistry and Biology of Trypanosomal Trans-Sialidases: Virulence Factors in Chagas Disease and Sleeping Sickness. *ChemBioChem* **2011**, *12*, 2246−2264.

(38) Alonso de Armiño, D. J.; Estrin, D.; Alvarez, R. M. S.; Roitberg, A. E. A Novel Conformational Switch Determines Trypanosoma Cruzi Trans Sialidase Activity at the Covalent Intermediate Stage. Submitted for publication in *Biochemistry*.

(39) Watts, A. G.; Damager, I.; Amaya, M. L.; Buschiazzo, A.; Alzari, P.; Frasch, A. C.; Withers, S. G. Trypanosoma cruziTrans-Sialidase Operates Through a Covalent Sialyl−Enzyme Intermediate: Tyrosine Is the Catalytic Nucleophile. *J. Am. Chem. Soc.* **2003**, *125*, 7532−7533.

(40) Bruner, M. Mechanistic Variation in the Glycosyltransfer of N-Acetylneuraminic Acid. *Nukleonika* **2002**, *47* (Suppl. 1), S25−S28.

(41) Mulholland, A. J. Computational Enzymology: Modelling the Mechanisms of Biological Catalysts. *Biochem. Soc. Trans.* **2008**, *36*, 22.

(42) Vanicek, J.; Mulholland, A. J. Computational Enzymology: Insight Into Biological Catalysts From Modelling. *Nat. Prod. Rep.* **2008**, *25*, 1001.

(43) Gao, J.; Ma, S.; Major, D. T.; Nam, K.; Pu, J.; Truhlar, D. G. Mechanisms and Free Energies of Enzymatic Reactions. *Chem. Rev.* **2006**.

(44) Lodola, A.; Sirirak, J.; Fey, N.; Rivara, S.; Mor, M.; Mulholland, A. J. Structural Fluctuations in Enzyme-Catalyzed Reactions: Determinants of Reactivity in Fatty Acid Amide Hydrolase From Multivariate Statistical Analysis of Quantum Mechanics/Molecular Mechanics Paths. *J. Chem. Theory Comput.* **2010**, *6*, 2948−2960.

(45) Senn, H. M.; Thiel, W. QM/MM Methods for Biomolecular Systems. *Angew. Chem., Int. Ed.* **2009**, *48*, 1198−1229.

(46) Hornak, V.; Abel, R.; Okur, A.; Strockbine, B.; Roitberg, A.; Simmerling, C. Comparison of Multiple Amber Force Fields and Development of Improved Protein Backbone Parameters. *Proteins* **2006**, *65*, 712−725.

(47) Cornell, W. D.; Cieplak, P.; Bayly, C. I.; Gould, I. R.; Merz, K. M.; Ferguson, D. M.; Spellmeyer, D. C.; Fox, T.; Caldwell, J. W.; Kollman, P. A. A Second Generation Force Field for the Simulation of Proteins, Nucleic Acids, and Organic Molecules. *J. Am. Chem. Soc.* **1995**, *117*, 5179−5197.

(48) de M Seabra, G.; Walker, R. C.; Elstner, M.; Case, D. A.; Roitberg, A. E. Implementation of the SCC-DFTB Method for Hybrid QM/MM Simulations Within the Amber Molecular Dynamics Package. *J. Phys. Chem. A* **2007**, *111*, 5655−5664.

(49) Capoferri, L.; Mor, M.; Sirirak, J.; Chudyk, E.; Mulholland, A. J.; Lodola, A. Application of a SCC-DFTB QM/MM Approach to the Investigation of the Catalytic Mechanism of Fatty Acid Amide Hydrolase. *J. Mol. Model.* **2011**, *17*, 2375−2383.

(50) Elstner, M. The SCC-DFTB Method and Its Application to Biological Systems. *Theor. Chem. Acc.* **2005**, *116*, 316−325.

(51) Krüger, T.; Elstner, M.; Schiffels, P.; Frauenheim, T. Validation of the Density-Functional Based Tight-Binding Approximation Method for the Calculation of Reaction Energies and Other Data. *J. Chem. Phys.* **2005**, *122*, No. 114110.

(52) Woodcock, H. L.; Hodoscek, M.; Brooks, B. R. Exploring SCC-DFTB Paths for Mapping QM/MM Reaction Mechanisms. *J. Phys. Chem. A* **2007**, *111*, 5720−5728.

(53) Barnett, C. B.; Naidoo, K. J. Ring Puckering: A Metric for Evaluating the Accuracy of AM1, PM3, PM3CARB-1, and SCC-DFTB Carbohydrate QM/MM Simulations. *J. Phys. Chem. B* **2010**, *114*, 17142−17154.

(54) Pierdominici-Sottile, G.; Roitberg, A. E. Proton Transfer Facilitated by Ligand Binding. An Energetic Analysis of the Catalytic Mechanism of *Trypanosoma cruzi* Trans-Sialidase. *Biochemistry* **2011**, *50*, 836−842.

(55) Darden, T. A. Y. D. P. L. Particle Mesh Ewald: an N·Log(N) Method for Ewald Sums in Large Systems. *J. Chem. Phys.* **1993**, *98*, 10089−10092.

(56) Kumar, S.; Rosenberg, J. M.; Bouzida, D.; Swendsen, R. H.; Kollman, P. A. THE Weighted Histogram Analysis Method for Free-Energy Calculations on Biomolecules. I. the Method. *J. Comput. Chem.* **1992**, *13*, 1011−1021.

(57) Doron, D.; Kohen, A.; Major, D. T. Collective Reaction Coordinate for Hybrid Quantum and Molecular Mechanics Simulations: A Case Study of the Hydride Transfer in Dihydrofolate Reductase. *J. Chem. Theory Comput.* **2012**, *8*, 2484−2496.

(58) Wong, K.-Y.; Gao, J. The Reaction Mechanism of Paraoxon Hydrolysis by Phosphotriesterase from Combined QM/MM Simulations. *Biochemistry* **2007**, *46*, 13352−13369.

(59) Major, D. T.; Gao, J. A Combined Quantum Mechanical and Molecular Mechanical Study of the Reaction Mechanism and *α*-Amino Acidity in Alanine Racemase. *J. Am. Chem. Soc.* **2006**, *128*, 16345−16357.

(60) Hensen, C.; Hermann, J. C.; Nam, K.; Ma, S.; Gao, J.; Höltje, H.-D. A Combined QM/MM Approach to Protein−Ligand Interactions: Polarization Effects of the HIV-1 Protease on Selected High Affinity Inhibitors. *J. Med. Chem.* **2004**, *47*, 6673−6680.

(61) Garcia-Viloca, M.; Truhlar, D. G.; Gao, J. Reaction-Path Energetics and Kinetics of the Hydride Transfer Reaction Catalyzed by Dihydrofolate Reductase. *Biochemistry* **2003**, *42*, 13558−13575.

(62) Dinner, A. R.; Blackburn, G. M.; Karplus, M. Uracil-DNA Glycosylase Acts by Substrate Autocatalysis. *Nature* **2001**, *413*, 752−755.

(63) Chatfield, D. C.; P Eurenius, K.; Brooks, B. R. HIV-1 Protease Cleavage Mechanism: A Theoretical Investigation Based on Classical MD Simulation and Reaction Path Calculations Using a Hybrid QM/MM Potential. *J. Mol. Struct.* **1998**, *423*, 79−92.

(64) Cunningham, M. A.; Ho, L. L.; Nguyen, D. T.; Gillilan, R. E.; Bash, P. A. Simulation of the Enzyme Reaction Mechanism of Malate Dehydrogenase. *Biochemistry* **1997**, *36*, 4800−4816.

(65) Davenport, R. C.; Bash, P. A.; Seaton, B. A.; Karplus, M.; Petsko, G. A.; Ringe, D. Structure of the Triosephosphate Isomerase-Phosphoglycolohydroxamate Complex: An Analog of the Intermediate on the Reaction Pathway. *Biochemistry* **1991**, *30*, 5821−5826.

(66) More, O'; Ferral, R. A. Relationships Between E2 and E1cB Mechanisms of Beta-Elimination. *J. Chem. Soc. B* **1970**, 274.

(67) Pauling, L. Atomic Radii and Interatomic Distances in Metals. *J. Am. Chem. Soc.* **1947**, *69*, 542−553.

(68) Houk, K. N.; Gustafson, S. M.; Black, K. A. Theoretical Secondary Kinetic Isotope Effects and the Interpretation of Transition State Geometries. 1. The Cope Rearrangement. *J. Am. Chem. Soc.* **1992**, *114*, 8565−8572.

(69) Lano, W. D. *PyMOL*, Version 0.99; Delano Scientific, URL: http://www.Pymol.org. *The PyMOL Molecular Graphics System*, Version 1.5.0.4; Schrödinger: Portland, OR, USA.

(70) Case, D. A.; Darden, T. A.; Cheatham, T. E., III; Simmerling, C.; Wang, J.; Duke, R. E.; Luo, R.; Walker, R. C.; Zhang, W.; Merz, K. M.; et al. *AMBER 12*; University of California: San Francisco, CA, USA, 2012.

(71) Roe, D. R.; Cheatham, T. E., III. PTRAJ and CPPTRAJ: Software for Processing and Analysis of Molecular Dynamics Trajectory Data. *J. Chem. Theory Comput.* **2013**, *9*, 3084−3095.

(72) Guthrie, R. D.; Jencks, W. P. IUPAC Recommendations for the Representation of Reaction Mechanisms. *Acc. Chem. Res.* **1989**, *22*, 343−349.

(73) IUPAC-IUB Joint Commission on Biochemical Nomenclature (JCBN). Conformational Nomenclature for Five- and Six-Membered Ring Forms of Monosaccharides and Their Derivatives: Recommendations 1980. *Eur. J. Biochem.* **1980**, *111*, 295−298.

(74) Oppezzo, P.; Obal, G.; Baraibar, M. A.; Pritsch, O.; Alzari, P. M.; Buschiazzo, A. Crystal Structure of an Enzymatically Inactive Trans-Sialidase-Like Lectin From Trypanosoma Cruzi: the Carbohydrate Binding Mechanism Involves Residual Sialidase Activity. *Biochim. Biophys. Acta* **2011**, *1814*, 1154−1161.

(75) Paris, G.; Cremona, M. L.; Amaya, M. F.; Buschiazzo, A.; Giambiagi, S.; Frasch, A. C. C.; Alzari, P. M. Probing Molecular Function of Trypanosomal Sialidases: Single Point Mutations Can Change Substrate Specificity and Increase Hydrolytic Activity. *Glycobiology* **2001**, *11*, 305−311.

■ NOTE ADDED AFTER ASAP PUBLICATION

This article posted ASAP on May 21, 2014. Changes have been made in sentence 2 of the Abstract; paragraph 7, sentence 8 of the Introduction section; equation 1; the caption of Figure 2; paragraph 2, sentence 2 of the Results and Discussion section, and Table 1. The corrected version posted on May 22, 2014.

5816

dx.doi.org/10.1021/jp412294r | *J. Phys. Chem. B* 2014, 118, 5807−5816